Investigations of an air-blown integrated gasification combined cycle fired with high-sulphur coal with post-combustion carbon capture by aqueous ammonia

Davide Bonalumi[a], Antonio Giuffrida[a*]

[a]Politecnico di Milano, Dipartimento di Energia, Via Lambruschini 4A, 20156 Milano, Italy

ABSTRACT

This work deals with CO_2 capture plants for an advanced air-blown gasification-based combined cycle where a coal with high sulphur content, which is really relevant for the coal market, is used as feedstock. The sulphur removed as H_2S from the coal-derived gas enters a wet sulphuric acid process. Later, the resulting acid is used to control ammonia slip in a post-combustion CO_2 capture plant based on ammonia scrubbing and designed for a reduced energy demand. Thus, limiting the energy impact of the CO_2 capture technology will improve the power plant efficiency, according to a presumable lower cost of the generated electricity, as a high-sulphur coal is used as fuel input.

In detail, a cooled ammonia-based process is found to be more attractive than a more conventional chilled ammonia-based solution: in case of 90% of CO_2 avoided, the overall power plant efficiency is equal to 41.7% and the SPECCA (specific primary energy consumption for CO_2 avoided) as low as 2.3 MJ/kg_{CO_2} . Moreover, the calculation results show the SPECCA for CO_2 avoided ranging from 80% to 90% is almost constant, even though the power plant efficiency increases if lower levels of CO_2 capture are considered.

1. Introduction

Coal is an abundant energy resource for electricity generation, with a lower cost than other fossil fuels. Coal-fired power plants are the main sources of electricity for emerging countries like China [1,2] and India [3,4], but suffer from poor acceptance by people in OECD (Organisation for Economic Co-operation and Development), mainly due to environmental issues. Currently, there are two main technical challenges for coal-fired power generation: the improvement of plant efficiency, as a way to reduce the cost of electricity, and the development of technologies such as CCS (carbon capture and storage) to reduce CO_2 emissions.

Dealing with pollutants emissions, it is necessary to remind that sulphur is one of the elements present in coal [5] and its content is really relevant to the coal market [6]. In particular, coal with sulphur content above 1% is classified as high-sulphur coal. The researchers' interest in the use of high-sulphur coal is actual as highlighted by very recent calculations of ultra-supercritical plants [7] and experiments on chemical looping combustion [8]

and pilot-scale gasification [9]. As a matter of fact, the IGCC (integrated gasification combined cycle) is a competitive technology to pulverized coal-fired steam power plants, with higher cycle efficiency as well as more effective removal of sulphide compounds from the coal-derived fuel gas, as removal efficiency values easily exceed 99%. The current IGCC technology is mainly based on oxygen-blown gasification, but a significant activity on air-blown IGCC has been conducting during the last years by Mitsubishi Heavy Industries in Japan, where the 250 MW_{el} demonstration plant in Nakoso was started up in 2007 [10]. Shifting from oxygen- to air-blown technology implies the eco-nomic advantage related to the much smaller air separation unit and the potentially higher cycle efficiency [11]. In perspective, IGCC efficiency values as high as 53% should be possible based on advanced technologies such as 1500°C-class combustion turbine and hot fuel gas clean-up [12].

In order to reduce CO_2 emissions significantly, carbon capture and storage are essential. There are three main capture technologies: post-combustion, pre-combustion de-carbonization and oxy-fuel combustion [13]. The concentration of CO_2 in the gas stream, the pressure of the gas stream and the fuel type (solid or gas) are

---

important factors in properly selecting the capture system, based on the specific process and the related engineering aspects [14]. Although the IGCC technology perfectly matches pre-combustion CO_2 capture [15], post combustion CO_2 capture solutions are worth of investigation, as reported by the authors [16,17] and by other researchers [18,19]. Indeed, post-combustion CO_2 capture is a feasible solution in the short term, as amine gas treating is a mature technology, with the alternative option of an ammonia-based process. However, independently of the specific technology, the energy cost related to CCS is not negligible and results in lower power plant performance [16–19].

1.1. Ammonia scrubbing for post-combustion CO_2 capture

In aqueous ammonia-based CCS technology, a rich CO_2 solution is produced in an absorber. The rich solution releases CO_2 at a relatively high pressure, when heated in a desorber, therefore the liquid is cooled and delivered to the absorber for a new cycle. Besides, the CAP (chilled ammonia process) layout is equipped with a water wash at the top of both the absorber and the regenerator, because of ammonia slip (NH_3 volatility results in NH_3 vaporization to the flue gas [20]), which is more significant for higher CO_2 absorption temperature.

Referring to real cases, lab-scale investigations of ammonia as a solvent have been conducted by Alstom [21] in 2005 and afterwards patented by Eli Gal [22] in 2006, operating in chilled conditions in order to avoid the ammonia slip. Alstom has licensed the exclusive world-wide rights to market and sell the patented CAP (chilled ammonia process) and has engaged in an extensive development and commercialization program. In 2008 a first pilot facility was installed at the We Energies plant in Pleasant Prairie and a second pilot plant, at the E.ON Karlshamn location in 2009, was applied to a high-sulphur fuel oil combustion. These plants have been run in chilled conditions, exploiting salt formation and adopting high regeneration pressure. In 2010 a larger plant has been investigated at AEP (American Electric Power's) Mountaineer plant [23], where a CAP plant has been designed to treat a 20 MW_{el} slipstream of combustion flue gases from an existing coal-fired boiler. Based on the results achieved with the first pilot plants, lower ammonia concentration has been considered as a fundamental process variable to avoid the solid formation, which is an issue investigated by several researchers [24–27]. Other developing activities are still ongoing [28–30].

Lots of technical papers on CAP-based CO_2 capture are present in the open literature. In particular, the authors' research group has gained a significant experience as regards (i) investigations of the design parameters for a CAP with a view to retrofitting an ultra-supercritical plant [31], (ii) energy and economic assessments of an ultra-supercritical plant integrated with CAP [32] and (iii) comparisons among different CAP-based plant layouts [33].

1.2. The ternary system $CO_2-NH_3-H_2O$

Understanding the phase behaviour and the thermodynamics of the $CO_2-NH_3-H_2O$ system [34] is important for engineers and researchers interested in post-combustion ammonia-based CO_2 capture. Such a ternary system forms an electrolyte solution, whose thermodynamic properties must be studied with an appropriate model.

The Extended UNIQUAC thermodynamic model proposed by Thomsen and Rasmussen [35] and later upgraded by Darde et al. [36] was used in this work. It is a local composition model derived from the original UNIQUAC model developed by Abrams and Prausnitz [37] and Maurer and Prausnitz [38], in which a Debye–Hückel term ac-counting for electrostatic interactions is added. Thus, the model al-lows for calculating the activity coefficients of electrolyte solutions.

The excess Gibbs energy is computed as the combination of three terms: a combinatorial (entropic) term, a residual (enthalpic) term and an electrostatic term [39]. The activity coefficients used for speciation, solid–liquid, and vapour–liquid equilibrium are calculated with the Extended UNIQUAC model. The Soave–Redlich–Kwong equation of state is employed for computing the fugacities of the species in the gas phase, without requiring additional adjustable parameter [39].

1.3. Objective of the paper

This work is a revised and extended version of an earlier conference paper [40] focussing on an original solution for firing high-sulphur coal in IGCC power plants for electricity generation with post-combustion CO_2 capture. In particular, an air-blown IGCC is considered and integrated with CO_2 capture processes, based on (i) a chilled and on (ii) a cooled aqueous ammonia scrubbing. This second solution aims at limiting the energy penalty related to the CCS technology, according to preliminary authors' investigations [17]. A strong integration between the desulphurization unit of the IGCC and the CCS plant is proposed. In detail, the ammonia slip is properly controlled and reduced to traces thanks to the H_2S removed from the coal-derived gas at the desulphurization unit of the IGCC.

2. Calculation environments

The thermodynamic models of the IGCC plants with CO_2 capture were implemented in the modular simulation code GS, integrated with the commercial code Aspen Plus®.

Mass and energy balances for the IGCC plants were carried out with the code GS [41], which is a simulation tool originally designed for research purposes by the authors' research group to calculate gas–steam cycles and progressively improved to calculate more complex systems. It has proved to yield highly accurate results in estimating the performance of combustion turbines and combined cycles [42] and has been successfully used to calculate mass and en-ergy balances of a variety of power plant configurations, including gasification systems, desulfurization reactors, water-gas shift pro-cesses as well as coal drying systems [43–48]. The main features of the code include: (i) the capability of reproducing very complex plant schemes by assembling basic modules, such as turbine, compressor, heat exchanger, etc., (ii) the use of built-in correlations for efficiency prediction of turbomachinery, as a function of the operating condi-tions, (iii) the use of built-in correlations to predict gas turbine cooling flows, (iv) the capability of calculating chemical equilibrium by Gibbs free energy minimization. Once the system to be calculated is defined as an ensemble of components, mass and energy balances of each component are calculated iteratively, until the conditions at all in-terconnections converge toward stable values.

The commercial code Aspen Plus® was used for the calculations of the CCS plant. In detail, the absorption and regeneration pro-cesses, better outlined in the next section, were simulated by means of the previously mentioned Extended UNIQUAC model that is not built inside the code but defined by the user, as successfully done by Darde et al. [39]. In particular, an exhaustive validation of the thermodynamic model was previously carried out and the model results compared with experimental data available in liter-ature [39]. Representative trends about this validation are shown in Figs. 1 and 2, based on experimental data by Kurz et al. [49] and limited to two temperatures of interest in an aqueous ammonia-based CO_2 capture process.[1] Besides, the Soave–Redlich–Kwong

---

[1] In addition to the comparisons reported by Darde et al. [39], further recent efforts are detailed in Ref. [50].
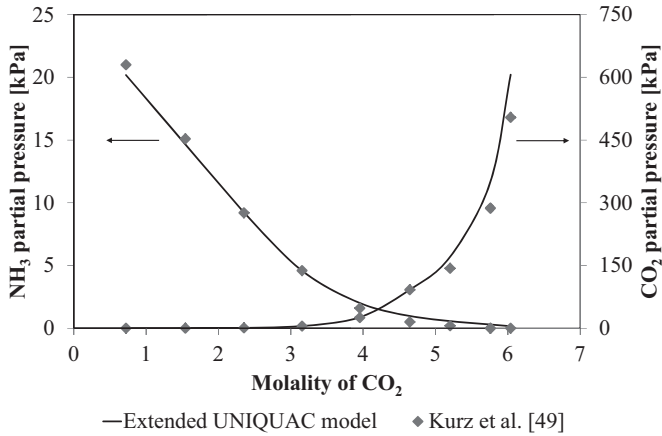
Fig. 1. Comparisons of the results at 313 K from the thermodynamic model Extended UNIQUAC with experimental data by Kurz et al. [49].
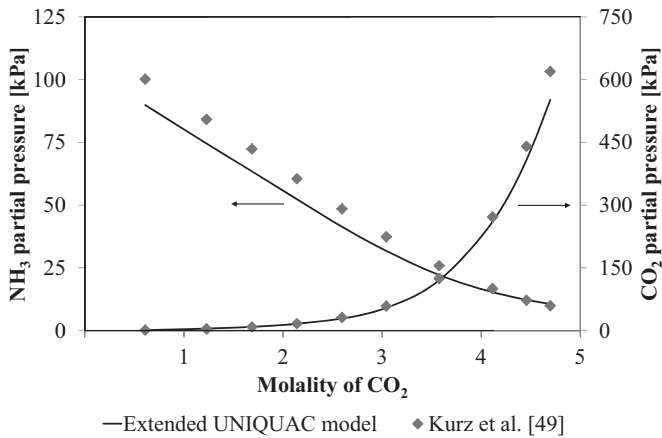

Fig. 2. Comparisons of the results at 353 K from the thermodynamic model Extended UNIQUAC with experimental data by Kurz et al. [49].

equation of state was chosen to simulate both the cooling of the gas entering the CCS plant and the CO_2 compression station.

Tables A1—A4 in the Appendix detail the main assumptions set for the calculations.

3. IGCC and CCS plant layouts

Each IGCC plant investigated in this work consists of two gasification islands and two combustion turbines with two heat recovery steam generators, which share the same steam turbine. Accordingly, two CCS plants are considered as the gas exiting each HRSG (heat recovery steam generator) unit is treated in a dedicated CCS plant. The IGCC and CCS plants are detailed in the following, with particular attention paid to the operation parameters of the CCS process as the result of a preliminary parametric analysis.

3.1. The IGCC plant

The schematic layout of the IGCC plant without CO_2 capture for the reference case is shown in Fig. 3. A high-sulphur Illinois #6 coal is considered as fuel input (with a lower heating value equal to 24.826 MJ/kg) and loaded by a dry lock hopper system by means of nitrogen from a dedicated stand-alone ASU (air separation unit). The oxygen delivered by the ASU is useful to enrich the O_2 content in the gasification stream. The air-blown coal gasification system, as

developed by MHI [51], is a water-wall entrained flow gasifier, with a combustor at the bottom and a reductor (the topper stage). Such a configuration allows for a carbon conversion of the order of 99.9% in the combustor [51], where coal and recycled char are burnt at high temperature (around 1900 °C) with high air-to-coal ratio. In the topper stage, high-temperature syngas is chemically quenched and experiences a temperature drop of around 700 °C. Because of the lower temperature, the coal-derived gas exiting the gasifier contains a certain amount of unconverted carbon, which is collected by a cyclone and recycled back to the combustor stage. As shown in Fig. 3, the air for coal gasification is extracted from the CT (combustion turbine) compressor outlet, partly cooled by producing HP (high pressure) steam and finally boosted to the gasification system. The coal-derived gas exiting the gasifier is firstly cooled down to 900 °C (11) before passing through cyclones, where char and ash are collected and recycled back to the combustor. Then, syngas is further cooled down to 350 °C (12) by producing HP steam and to 206.6 °C by preheating the clean syngas (17) up to 250 °C, before combustion. The removal of entrained ash and of soluble contaminants is realized by syngas scrubbing. A regenerative heat exchanger is used to heat the syngas from the scrubber (15) up to the operating temperature of a catalytic reactor for converting COS into H_2S. Hydrolyzed syngas stream is then cooled down to near-ambient temperature by pre-heating: (i) scrubbing water, (ii) water for the bottoming steam cycle directed to the deaerator and (iii) desulfurized syngas from the AGR (acid gas removal) station, where H_2S removal is carried out by means of a methyl diethanolamine-based process. After the AGR station, the clean syngas is heated up and burned in the CT combustor of an advanced CT unit, with the turbine inlet tempera-ture set at 1360 °C [52]. Thanks to the high N_2 content in the syngas fuelling the combustion turbine, no saturation with water is neces-sary to obtain a stoichiometric flame temperature compatible with acceptable NO_x emissions at the turbine exhaust [53]. Ultimately, the CT exhaust heat is recovered in a two pressure level steam cycle with reheat. Details of streams numbered in Fig. 3 are reported in Table 1, based on IGCC calculations.

The lay-out of the IGCC plant with CO_2 capture is strictly similar to the one in Fig. 3, with a few exceptions.

- Part of the carbon dioxide delivered by the CO_2 compressor at the CCS plant is recycled back to the gasification island for coal loading (see Figs. 4 and 5). Carbon dioxide is recommended in applications involving CO_2 removal [54,55], since it is available at no additional costs. Thus, the availability of CO_2 as an inert for coal loading makes the ASU unnecessary.[2]
- As the air blown to the gasifier is not oxygen-enriched, using CO_2 instead of N_2 for coal loading results in slight variations in the cold gas efficiency:

$$CGE = \frac{\dot{m}_{syngas} \cdot LHV_{syngas}}{\dot{m}_{coal} \cdot LHV_{coal}} \tag{1}$$

- In detail, this figure is equal to 73.07% and 72.5% in the plants without and with CO_2 capture, respectively. Thus, slight variations in stream details compared to those in Table 1 are calculated,[3] but they do not invalidate the comparison between the IGCC cases without and with CO_2 capture.

---

[2] As a matter of fact, the main duty of the ASU in an air-blown IGCC is delivering nitrogen for coal loading, while oxygen enrichment of the gasification stream is a secondary result [51].

[3] In particular, the gas exiting the HRSG units in IGCC systems with post-combustion CO_2 capture presents the following composition (on a molar basis): 0.89% Ar, 9.97% CO_2, 4.36% H_2O, 75.10% N_2, 9.68% O_2.
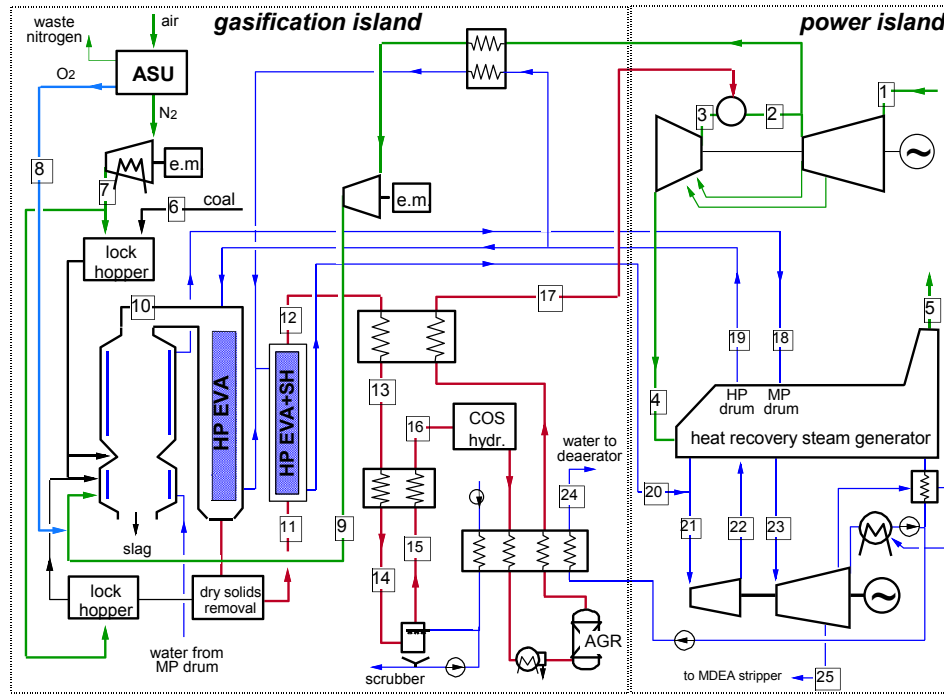
Fig. 3. Schematic of the IGCC plant (reference case without CO_2 capture).

Table 1
Temperature, pressure, flow rate and composition of the main streams of the air-blown IGCC shown in Fig. 3.

	T (°C)	p (bar)	ṁ (kg/s)	Ar	CO	CO_2	H_2	H_2O	H_2S	N_2	O_2	CH_4
1	15	1.01	611	0.92		0.03		1.03		77.28	20.73	
2	417.6	18.16	378.8	0.92		0.03		1.03		77.28	20.73	
3	1438.8	17.61	540	0.89		10.62		5.65		75.24	7.6	
4	611.1	1.04	665	0.89		8.59		4.77		75.63	10.12	
5	115	1.01	665	0.89		8.59		4.77		75.63	10.12	
6	15		39.1	Coal as received (%wt.: 61.27 C, 4.69 H, 8.83 O, 1.1 N, 3.41 S, 12 moisture, 8.7 ash)								
7	80	56.13	19.9							100		
8	15	35	7.3	3.09						1.91	95	
9	477.4	33.02	107.1	0.92		0.03		1.03		77.28	20.73	
10	1200	28.06	172.4	0.61	25.28	3.62	11.91	4.22	0.62	53.19		0.56
11	900	28.06	170	0.61	25.28	3.62	11.91	4.22	0.62	53.19		0.56
12	350	27.5	170	0.61	25.28	3.62	11.91	4.22	0.62	53.19		0.56
13	206.6	26.95	170	0.61	25.28	3.62	11.91	4.22	0.62	53.19		0.56
14	137	26.41	170	0.61	25.28	3.62	11.91	4.22	0.62	53.19		0.56
15	112	25.89	172.2	0.60	24.83	3.56	11.7	5.92	0.60	52.24		0.55
16	180	25.37	172.2	0.60	24.83	3.56	11.7	5.92	0.60	52.24		0.55
17	250	23.16	161.2	0.64	26.74	2.93	12.6	0.24		56.26		0.59
18	250	36	8.1					100				
19	339	144	106.9					100				
20	565	144	106.9					100				
21	560.6	132.5	316.8					100				
22	359.6	36	313.7					100				
23	563.8	33.12	329.9					100				
24	100	2	89.4					100				
25	191.2	2	15.6					100				

- More steam is extracted from the bottoming cycle in case of CO_2 capture. In detail, stream 25 in Fig. 3 has to supply (i) the heat for H_2S stripping at the AGR station and (ii) the heat required at the CCS plant for the regeneration of the CO_2-rich solution, accomplished with CO_2 release, and for NH_3 strip-ping, if necessary. Such an increased steam extraction will reflect on reduced power output from the bottoming cycle.
- The H_2S removed (around 1.4 kg/s from each gasification is-land) from the raw coal-derived gas at the AGR station is not

recovered in a Claus plant [56], but used as input in a wet sulphuric acid process, as better detailed in the following.

3.2. The CCS plant in chilled mode

As schematized in Fig. 4, the gas stream exiting the HRSG is chilled in a first section of the plant with three contact coolers in cascade at decreasing temperature levels: the first system
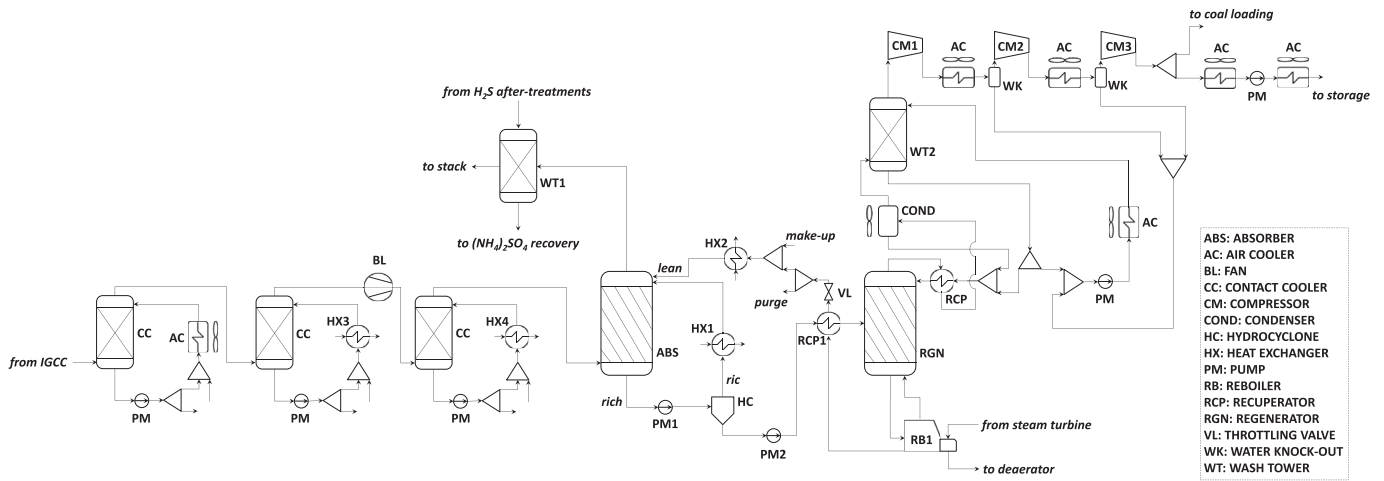
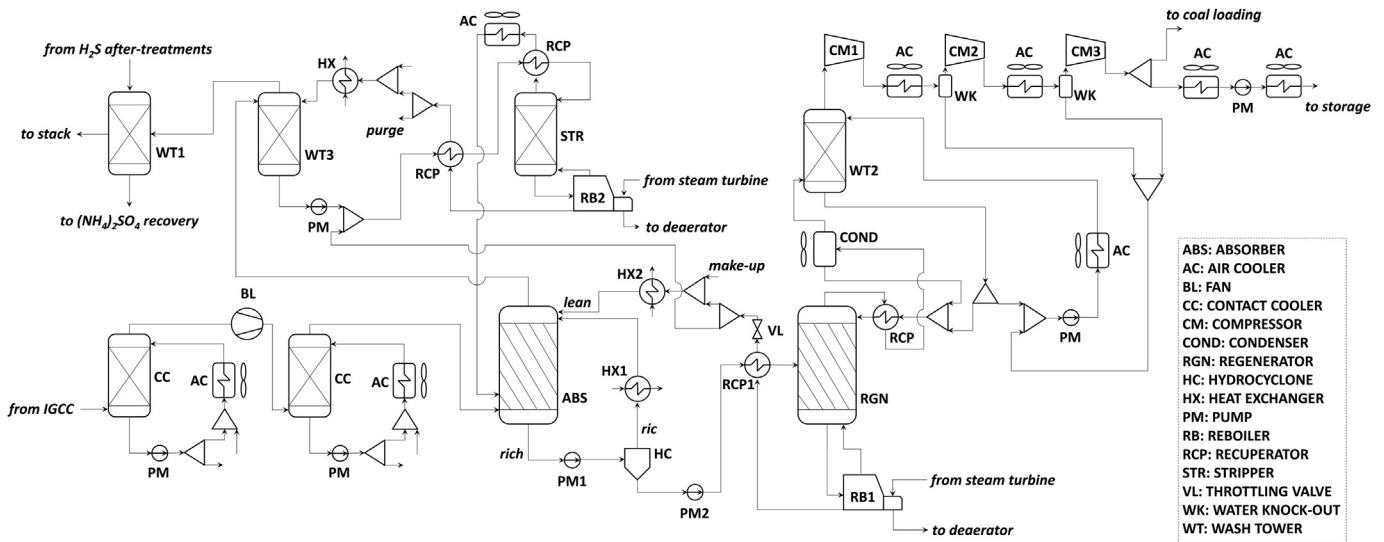**Fig. 4.** Schematic of the CCS plant for the chilled case.

Fig. 5. Schematic of the CCS plant for the cooled case.

operates with an ambient air-cooled water loop and the other two with chilled water loops (HX3 and HX4). The evaporation temperature of the chillers is set as low as possible, with prevention of ice formation (the gas from the HRSG releases moisture when passing through the contact coolers). As the gas flowing through the three contact coolers and the next absorber experiences a pressure drop, a fan (BL) is present. The gas temperature rise (no more than 7 °C) due to the fan is promptly reduced by the third contact cooler, before the gas enters the CO_2 absorption section, whose layout is conventional and similar to the one proposed in Ref. [33].

The CCS plant consists of an absorber and a regenerator with a recuperative heat exchanger (RCP1) as well as a high-pressure pump (PM2) for the rich solution to the regenerator and a chilling exchanger (HX2) on the lean solution to the absorber. All the streams entering the absorber are chilled at 7 °C. The absorber temperature varies through the reactor from around 7 °C (at the top) to 16 °C (at the bottom), due to the exothermic reactions. The rich solution from the absorber is pumped to a hydrocyclone, which separates the solids, sent to regeneration with a small portion of liquid, from the bulk of the liquid, chilled in HX1 and recycled back

to the absorber in order for the process temperature to be as cold as possible, being the absorption reaction exothermal. The ammonia slipping from the absorber wash is reduced to traces by acid washing in a dedicated tower (WT1). In detail, the H_2S-rich stream stripped after solvent regeneration at the desulphurization unit of the IGCC is supposed to react with air,[4] according to the following reaction (the presence of N_2 and other inerts in air is neglected for the sake of simplicity):

$$H_2S + \frac{3}{2} O_2 \rightarrow SO_2 + H_2O \qquad (2)$$

After SO_2-to-SO_3 oxidation in presence of a vanadium oxide catalyst, hydration and condensation, H_2SO_4 is ready to be used in order to drastically reduce ammonia slip in the stream exiting the absorption section, according to the following reaction:

---

[4] Based on the H_2S content (around 40%) in the gas from the AGR station, no feed air preheating or oxygen enrichment have to be used to maintain a stable temperature within the flammability limits [57,58].

$$2NH_3 + H_2SO_4 \rightarrow (NH_4)_2SO_4 \qquad (3)$$

The heat released with H_2S oxidation and the other exothermic reactions in the wet sulphuric acid process was preliminarily ignored in the next calculations.

In such a chilled mode, ammonia slip is limited, so it can completely react with the H_2S from the desulphurization unit and no after-treatment NH_3 capture is necessary.

As regards the path of the CO_2 stream exiting the regenerator, a condenser for moisture separation, operating with a dedicated air cooler, and a water wash tower (WT2) for ammonia slip control, with an air-cooled closed loop, are present. Finally, there is the CO_2 compression station, which consists of air-cooled stages with the same pressure ratio (CM1 to CM3), intercoolers and condensed water knockouts to dehydrate the CO_2 stream. CO_2 enters the compression station at a pressure depending on regeneration conditions and exits the last stage at slightly supercritical pressure. After recycling the amount of CO_2 necessary for coal loading and a further cooling, the supercritical liquid CO_2 stream is ultimately pumped to storage.

3.3. The CCS plant in cooled mode

The layout in Fig. 5 for the CCS plant in cooled mode is very similar to the one in Fig. 4. However, four main differences have to be pointed out.

- When cooling the gas exiting the HRSG unit, two contact coolers are sufficient with no chiller.
- All the streams entering the absorber are cooled down to 20 °C. Because of the exothermic reactions, the absorber temperature varies through the reactor from around 20 °C (at the top) to 25 °C (at the bottom). The temperature of 20 °C for the streams entering the absorber is selected based on 15 °C of ambient temperature. As reported in Fig. 5, air-coolers replace the chilling system.
- The operation temperature of the absorber is higher, which increases the solubility of the salts present in the system, as also showed by other researchers [30]. This condition, alone, is not enough to avoid the precipitation of salts a priori, so a hydrocyclone is always present in the layout of Fig. 4.

Ammonia slip in cooled mode is significant, so an absorption−desorption cycle just before the final acid washing (WT1) is necessary for a level of ammonia slip reducible by the H_2S available from the desulphurization unit of the IGCC, as previously described. In particular, part of the NH_3 in the gaseous stream exiting the absorber is firstly reduced in a wash tower (WT3), resulting in a NH_3-rich solution pumped from the wash tower to a stripper, where NH_3 in the gaseous phase is recovered and delivered to the absorber.

3.4. Operation parameters for the CCS plants

Six operation parameters were considered when running simulations of the CCS plants in both the chilled and cooled modes (see Table 2):

- the temperature of the streams entering the absorber (in chilled or cooled mode),
- the amount of CO_2 captured,
- the ammonia initial concentration (conc) in the aqueous solution:

$$conc = \left. \frac{\dot{m}_{NH_3}}{\dot{m}_{NH_3} + \dot{m}_{H_2O}} \right|_{lean} \qquad (4)$$

- the NH_3-to-CO_2 ratio in the absorber (K), defined as the ratio between the number of NH_3 moles in the lean solution line to the absorption reactor and the number of CO_2 moles in the line from the HRSG outlet:

$$K = \frac{\dot{n}_{NH_3, \ lean}}{\dot{n}_{CO_2, \ in}} \qquad (5)$$

- the percentage of rich solution recycled (ric) to the absorber,
- the regeneration pressure.

The CCS plant simulations were carried out at the equilibrium in order to evaluate the potential performance of the processes here proposed. The values reported in Table 2 were fixed for the preliminary investigations of energy demand by the CCS plant. Further details on other parameters assumed for CCS simulations are reported in the Appendix (see Table A4).

Focussing on the two CCS modes, three levels of CO_2 capture (i.e. 80%, 85% and 90%) were considered for the cases presented and discussed in the next section. Cases with CO_2 capture less than 80% were not investigated in this work, even though techno-economic considerations are always necessary to set a proper target of CO_2 capture.

Due to NH_3 volatility, it is necessary for the absorption temperature to be as low as possible. Thus, 7 °C is selected as the minimum temperature to avoid ice formation in chilled mode. Based on the ambient temperature (15 °C), 20 °C is selected as the minimum temperature in cooled mode, with air-coolers replacing the chilling system. In addition, setting the temperature of the streams entering the absorber directly affects (i) the temperature for the exhaust gas treatments, (ii) the flow rate of the lean solution and (iii) the amount of the rich solution recycled to the absorber (ric in both Figs. 4 and 5). On the other hand, setting a regeneration pressure requires to operate at a specific temperature for a fixed level of CO_2 capture.

All the investigated cases in chilled mode are characterized by the precipitation of solids, due to the lower temperature in the absorber. The solution containing solids can be handled similarly as in flue gas desulfurization plants, usually equipped with open spray tower or absorber tray system and slurry pumps, made of corrosion- and wear-resistant metal as well as rubber materials.
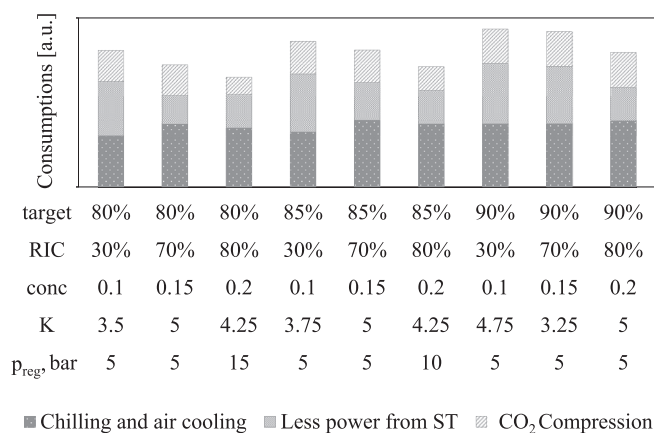
Referring to the most significant energy consumptions, Fig. 6 shows a comparative overview of some representative cases for the CCS plant in chilled mode, purposely limited for the sake of conciseness. In detail, based on the experience achieved with former works [32,33], a significant number of cases was investigated as parametric simulation runs. Ultimately, after fixing the CCS mode and the level of CO_2 capture, the values of the last four pa-rameters in Table 2 were selected as their combination allowing for the lower energy cost. Accordingly, Table 3 reports these values as the results of the preliminary analysis (CH and CO stand for chilled and cooled mode, respectively, whereas 80, 85 and 90 refer to the level of CO_2 capture). As detailed in Table 3, different sets of parameter values were found for the three cases in chilled mode, whereas the same set of values was found for cases CO-85 and CO-90, in cooled mode, differently from case CO-80.

The analysis of CCS plants simulated based on the parameter values reported in Table 2 allowed to better understand the response of the CCS plant as a function of the specific parameter

Table 2
Preliminary assumptions for the investigated parameters of the CCS plants.

Parameter	Values
Temperature of the streams entering the absorber, °C	7, 20
Amount of CO_2 captured, %	80, 85, 90
NH_3 initial concentration (conc), kg/kg	0.05, 0.1, 0.15, 0.2
NH_3-to-CO_2 ratio (K), mol/mol	4, 4.5, 5, 5.5, 5.75
Recycled rich solution (ric), %	10, 20, 30, 40, 50, 60, 70, 80, 90
Regeneration pressure, bar	5, 10, 20

target	80%	80%	80%	85%	85%	85%	90%	90%	90%
RIC	30%	70%	80%	30%	70%	80%	30%	70%	80%
conc	0.1	0.15	0.2	0.1	0.15	0.2	0.1	0.15	0.2
K	3.5	5	4.25	3.75	5	4.25	4.75	3.25	5
p_{reg}, bar	5	5	15	5	5	10	5	5	5

■ Chilling and air cooling ▨ Less power from ST ▨ CO_2 Compression

Fig. 6. Comparative overview of the energy consumptions (in arbitrary units) for the CCS plant in chilled mode, based on the amount of CO_2 captured (target) and four process parameters.

Table 3
Key-parameters assumed for CCS plant calculations.

	CH-80	CH-85	CH-90	CO-80	CO-85	CO-90
ric, wt%	80	80	80	50	10	10
conc, wt%	20	20	20	10	5	5
K, mol/mol	4	4.25	5	5.25	4.75	4.75
Regeneration pressure, bar	15	10	5	5	5	5

variation. As a result of the parametric analysis, the following considerations can be reported as guidelines to limit the energy cost related to the CCS process.

- Lower regeneration pressures are favourable in case of cooled mode since the difference between the rich and lean loadings is higher than in case of chilled mode. Thus, more energy can be saved as lower quality heat is necessary in the regeneration stage.
- Higher regeneration pressures are favourable when decreasing the level of CO_2 capture in case of chilled mode since a lower difference between the rich and lean loadings is necessary and more energy can be saved in the compression stage.
- Higher recirculation ratios of the rich-solution are necessary for the CH cases, owing to the higher concentrations of ammonia (20%). As a matter of fact, a higher recirculation ratio causes lower ammonia slip, which reflects on lower energy required for the ammonia recovery.
- The values of the NH_3-to-CO_2 ratio in the absorber, as reported in Eq. (5), increase in case of chilled mode and decrease when switching to the cooled mode. They are justified as more ammonia is required since the lean loading is higher than in the case of cooled mode.

In addition, the lean loading for the CCS plants investigated in chilled mode resulted around 0.6, with a variation of the rich loading from 0.7 to 0.8. In case of cooled mode, the lean and rich loading resulted around 0.4 and 0.7, respectively.

On the whole, relatively similar results can be obtained with both the layouts. Nevertheless, the CH cases would require unconventional solutions to solve the problems related to salt precipitation. As a matter of fact, according to the specific parameters in Table 3, the simulated CH cases suffer this drawback, because of pursuing an energy cost as low as possible. On the other hand, the temperature reached in the absorber in case of cooled mode allows to avoid solid formation, resulting in a simpler plant to run. In particular, a packed column, with a reduction in the size of the absorber, can be adopted along with common pumps and the hydrocyclone could be avoided.

4. Results and discussion

The results of the IGCC calculations are here presented and discussed with reference to power balances and overall IGCC performance. In detail, the size of the IGCC plant depends on the CT technology at the topping cycle, with the assumed mass flow rate at the CT outlet (see Table A2).

Preliminarily, attention is paid to the results in Table 4, where power details for the gasification island components and for the topping cycle of the IGCC plant without and with CO_2 capture are reported. As previously anticipated, in case of CO_2 capture, part of the captured and compressed carbon dioxide is used for coal loading. Thus, neither ASU nor lock-hopper compressors are present, the air entering the gasifier is not oxygen-enriched and the air booster is unavoidably bigger to blow the amount of oxygen required for coal gasification. Accordingly, CT compressor power slightly increases, reflecting on less power output from the topping cycle.

Focussing on the bottoming cycle and on the after-treatment station, power details are reported in Tables 5 and 6.

The following results for the IGCC plants with CO_2 capture in chilled mode are worth of attention.

- The power output from the steam turbine reduces because of steam extraction related to the heat duty of the regenerator.
- The heat rejected at the condenser is almost halved because of less steam expanding through the LP (low pressure) stages of the turbine.
- The power required by the condenser pump is directly related to the condenser duty. However, the overall power requirement by HRSC (heat recovery steam cycle) pumps reduces less than the heat rejected at the condenser, as the duty of feedwater pumps is almost unchanged due to negligible variations in the amount of water pumped from the condenser and the reboilers.
- The same power for exhaust cooling is required, before the gas enters the CO_2 absorber.
- At the CO_2 capture plant, the heat duty of the regenerator reduces when less CO_2 is removed from the flue gas (from case CH-90 to case CH-80), even though the operation temperature at the regenerator slightly raises for lower CO_2 capture levels, as a consequence of the regeneration pressure (see Table 3). In case of higher levels of CO_2 capture, the number of reacting moles increases, so power requirements for chilling and air cooling raise (the CO_2 chemical absorption is an exothermic process), whereas pumping power nearly halves from case CH-80 to case CH-90, due to the specific regeneration pressure.
- Different CO_2 compression energy costs in Table 5 depend both on the amount of CO_2 captured and on the CO_2 pressure at the inlet of the compression system.

Table 4
Power details for the gasification island components and the topping cycle of the IGCC plants without and with CO_2 capture.

	IGCC without capture	IGCC with capture
Air separation unit, MW_{el}	10.5	–
Lock hopper compressors, MW_{el}	10.2	–
Air booster, MW_{el}	14.9	19.5
Gasification island auxiliaries, MW_{el}	5.3	5.4
CT compressor, MW_{el}	247.9	255.0
CT expander, MW_{el}	524.5	520.6
CT generator loss and auxiliaries, MW_{el}	4.6	4.4

Table 5
Power details for the bottoming steam cycle and the CCS plant (the latter just for one gasification train) in chilled mode.

	REF	CH-80	CH-85	CH-90
Steam turbine, MW_{el}	501.1	476.4	476.7	474.1
HRSC pumps, MW_{el}	13.0	10.6	10.4	10.2
Heat rejected at the condenser, MW	641.1	379.8	356.9	337.8
Exhaust cooling				
Air cooler and chillers, MW_{el}	–	7.6	7.6	7.6
Fan, MW_{el}	–	5.9	5.9	5.9
Pumps, MW_{el}	–	0.2	0.2	0.2
CO_2 capture plant				
Heat duty at the regenerator, MW	–	171.5	182.8	193.7
Regeneration temperature, °C	–	74.4	71.1	67.4
Chillers and air cooler, MW_{el}	–	32.9	35.1	36.9
Pumps, MW_{el}	–	1.9	1.4	1.0
CO_2 compression				
IC compressors and pump, MW_{el}	–	9.3	12.8	19.0
Air coolers, MW_{el}	–	0.5	0.5	0.7
Overall results				
Gross electric power output, MW_{el}	1047.0	1000.8	1001.1	998.4
IGCC plant auxiliaries, MW_{el}	96.9	74.3	74.1	73.9
CCS plant auxiliaries, MW_{el}	–	116.5	127.2	142.6
Net electric power, MW_{el}	950.1	809.9	799.8	781.9
Net electric LHV efficiency, %	48.93	41.30	40.78	39.87
Specific emissions, kg_{CO_2}/MWh	647.7	174.8	133.9	91.6
SPECCA, MJ/kg_{CO_2}	–	2.88	2.86	3.01

Paying attention to the overall results in Table 5 and moving from case CH-90 to case CH-80, it is possible to appreciate an obvious increase in net power output and LHV efficiency. However, the incremental improvements are more interesting from case CH-90 to case CH-85 than from case CH-85 to case CH-80. As a matter of fact, referring to the SPECCA (specific primary energy consumption for CO_2 avoided) defined as:

$$SPECCA = \frac{3600 \cdot \left(\frac{1}{\eta} - \frac{1}{\eta_{ref}} \right)}{ER_{ref} - ER} \quad (6)$$

the minimum value seems to be calculated just for case CH-85, as no significant difference is appreciated for case CH-80. Based on these results and referring to the performance of air-blown IGCC plants with pre-combustion CO_2 capture [46,48], chilled ammonia scrubbing does not seem to be a particularly attractive technology, even though it is a solution worthy of investigation, with a SPECCA lower than conventional amine-based CCS [16].

On the other hand, switching attention to the results reported in Table 6 for the CCS cases in cooled mode, IGCC performance is completely different. Four cases are reported in Table 6: the first three refer to cases from CO-80 to CO-90, according to calculations based on the parameters detailed in Table 3, whereas the fourth case is included for next comparisons. Such an additional case, namely CO-80*, is characterized with the same parameters found and set for both cases CO-85 and CO-90 (see Table 3).

Apart from considerations similar to the ones for the cases in chilled mode, proper attention should now be paid to the presence of the NH_3 stripper and its related heat duty. As a matter of fact, controlling ammonia slip reflects on the overall energy demand of the CCS plant.[5] Paying attention to the heat duty at the NH_3 stripper, a singular trend may be appreciated if considering the first three cases in Table 6. As far as the heat duty at the NH_3 stripper is concerned, focus on cases CO-80*, CO-85 and CO-90 would be necessary for a more consistent comparison.[6] Nevertheless, the overall performance of the CCS plant for case CO-80 is better than for case CO-80*, as resulting from the preliminary parametric analysis.[7] The results reported in Table 6, with the supplementary case CO-80*, point out that proper setting the parameters in Table 3, here arranged according to the preliminary parametric analysis, is really important in order to reduce the energy cost introduced with the CCS plant, notwithstanding the limited variations in overall IGCC performance.

Although NH_3 concentration in the flue gas is sensibly higher in CO cases and a NH_3-removal section before the final acid wash is necessary (the amount of H_2S removed at the AGR station of the IGCC is not sufficient to completely reduce NH_3 to traces), the SPECCA value is almost constant and definitely lower than the ones calculated for the cases in chilled mode. This performance index highlights how much promising the proposed CCS technology in cooled mode is for the IGCC power plant here investigated. As a matter of fact, a previous study of amine-based CCS technology in similar IGCC plants resulted in a SPECCA around 3.1 MJ/kg_{CO_2} [16], higher than the values detailed in Table 6. Ultimately, as a comparison between coal-fired power plants, the SPECCA related to the proposed CCS technology in cooled mode results as low as the ones reported for pulverized-coal steam cycles integrated with a piperazine-based CCS process (around 2.3 MJ/kg_{CO_2}) [59].

5. Conclusions

An original way to effectively use low-price coal for electricity generation with reduced CO_2 emissions has been proposed. The integration between an advanced air-blown IGCC, fired with high-sulphur coal, and a post-combustion ammonia-based CCS plant was assessed. Based on a preliminary parametric investigation, optimum conditions were defined for three levels of CO_2 capture (from 80% to 90%). In particular, two CCS operation modes were fixed in order to evaluate a first chilled and a second cooled case, with specific key-parameters finely tuned for the investigated plant. The ammonia slip, which is the main drawback related to ammonia-based CCS technology, is here controlled and reduced to traces by acid wash with the H_2S recovered in the desulphurization unit of the IGCC, resulting in ammonium sulphate, which is a valuable fertilizer.

Compared to the case with no CO_2 capture, IGCC efficiency reduces from 7.6 to 9.1 and from 6.3 to 7.2 percentage points when increasing CO_2 capture, in chilled and cooled mode, respectively. Moreover, based on a cooled ammonia-based CCS technology, an almost constant specific primary energy consumption for CO_2 avoided was calculated as low as 2.27 MJ/kg_{CO_2}, independently from the amount of CO_2 captured in the investigated range from 80% to 90%. Thus, the ammonia-based CCS technology reveals itself

---

[5] Ammonia slip is less evident for the CH cases, where the lower absorber temperature prevents large NH_3 slipping in the gas phase and the final acid wash is sufficient to reduce NH_3 to traces.

[6] The heat duty of 10.4 MW for case CO-80* outlines a clear trend with the other corresponding values for cases CO-85 and CO-90.

[7] The larger heat duty at the NH_3 stripper for case CO-80 is justified by larger ammonia slip than in the other three cases reported in Table 6. As a matter of fact, ammonia initial concentration (conc) in the aqueous solution for case CO-80 is twice the same parameter for cases CO-85 and CO-90 (see Table 3).

Table 6
Power details for the bottoming steam cycle and the CCS plant (the latter just for one gasification train) in cooled mode.

	REF	CO-80	CO-85	CO-90	CO-80*
Steam turbine, MW_{el}	501.1	446.0	438.8	433.1	443.5
Steam cycle and condenser HRSC pumps, MW_{el}	13.0	10.2	9.9	9.7	10.1
Heat rejected at the condenser, MW	641.1	340.2	310.3	285.8	329.1
Exhaust cooling					
Air cooler and chillers, MW_{el}	–	0.8	0.8	0.8	0.8
Fan, MW_{el}	–	5.5	5.5	5.5	5.5
Pumps, MW_{el}	–	1.1	1.1	1.1	1.1
CO_2 capture plant					
Heat duty at the regenerator, MW	–	177.3	210.1	221.7	199.6
Regeneration temperature, °C	–	104.6	105.3	106.5	104.2
Heat duty at NH_3 stripper, MW	–	29.4	13.6	18.8	10.4
Temperature for NH_3 stripping, °C	–	97.0	97.8	97.9	97.8
Chillers and air cooler, MW_{el}	–	3.91	3.85	4.31	3.52
Pumps, MW_{el}	–	1.4	2.0	2.0	2.0
CO_2 compression					
IC compressors and pump, MW_{el}	–	16.7	17.8	18.9	16.7
Air Coolers, MW_{el}	–	0.6	0.6	0.6	0.6
Overall results					
Gross electric power output, MW_{el}	1047.0	970.3	963.1	957.5	967.8
IGCC plant auxiliaries, MW_{el}	96.9	73.9	73.6	73.3	73.8
CCS plant auxiliaries, MW_{el}	–	60.1	63.3	66.4	60.6
Net electric power, MW_{el}	950.1	836.4	826.3	817.7	833.4
Net electric LHV efficiency, %	48.93	42.64	42.13	41.69	42.49
Specific emissions, kg_{CO_2}/MWh	647.7	170.3	127.9	86.4	170.5
SPECCA, MJ/kg_{CO_2}	–	2.27	2.29	2.27	2.34

more attractive in cooled than in chilled mode. However, this result is strictly related to the case investigated here, i.e. when firing high-sulphur coal in IGCC plants. As a matter of fact, in case of gasifica-tion of more common low-sulphur bituminous coal [60], perfor-mance results of IGCC plants with the same CCS technology are not so clear as the ones presented in this paper.

Ultimately, the promising results presented here are worthy of further investigations. In detail, the kinetics of the process should be implemented to dimension the CCS plant components for an eco-nomic assessment of the proposed CO_2 capture technology. Attention could also be paid to the heat recovery from H_2S combustion, though limited, with possible integration for CO_2 and/ or NH_3 stripping.

Appendix

The following tables detail the main assumptions for IGCC calculations.

Table A1
Main assumptions for gasification island calculations.

Gasification pressure, bar	28.06
Combustor/reductor temperature, °C	1900/1200
Heat to membrane walls, % of input coal LHV	2
Air booster polytropic efficiency, %	90.5
Heat loss in syngas coolers, % of transferred heat	0.7
Pressure loss in syngas coolers, %	2
Steam consumption at AGR station, MJ of steam at 2 bar per kg of removed H_2S	26.22
AGR auxiliaries, MJ_{el}/kg_{H2S}	1.11
Coal milling and handling, kJ_{el}/kg_{coal}	50
Slag handling, kJ_{el}/kg_{ash}	100
BOP, % of input coal LHV	0.15

Table A2
Main assumptions for combustion turbine calculations.

Air pressure loss, %	1
Compressor pressure ratio	18.1
Compressor polytropic efficiency, %	92.25
Compressor leakage, % of the inlet flow	0.75
Fuel valve pressure loss, bar	5
Cooled/Uncooled turbine stage isentropic efficiency, %	91.5/92.5
Turbine inlet temperature, °C	1360

Table A2 (*continued*)

Heat loss at combustor, % of fuel LHV	0.9
Mass flow rate at CT outlet, kg/s	665
CT auxiliaries, % of gross power	0.35
Turbine/compressor mechanical efficiency, %	99.865
Electric generator efficiency, %	98.7

Table A3
Main assumptions for HRSC calculations.

HRSG gas side pressure loss, kPa	3
Heat loss, % of transferred heat	0.7
HP/MP level, bar	144/36
Maximum live steam temperature, °C	565
Minimum pinch point ΔT, °C	10
Subcooling ΔT, °C	5
Minimum stack temperature, °C	115
Pressure losses in HP/MP economizers, bar	16/25
Pressure loss in superheaters, %	8
Condensing pressure, kPa	4
Power for heat rejection, MJ_{el}/MJ_{th}	0.01
Pumps hydraulic efficiency, %	80
Turbine mechanical efficiency, %	99.5
Electric generator efficiency, %	98.7

Table A4
Main assumptions for CCS plant calculations.

CO_2 capture plant	
Fluid temperature at air-cooler outlet, °C	25
Pressure drop in air-coolers, %	1
Specific consumption for heat rejection by air-cooling, $kW_{el} \cdot MW^{-1}$	15.9
Pinch point ΔT in heat exchangers, °C	5
Coefficient of performance for chilling, $MW \cdot MW_{el}^{1}$	5
Fan polytropic efficiency, %	0.85
Fan pressure ratio	1.1
Pumps hydraulic/mechanical-electric efficiency, %	80/95
Pressure drop in contact coolers, bar	0.01
Pressure drop in columns, bar	0.03
Maximum ammonia in CO_2 to storage, $mg \cdot Nm^{-3}$	10
CO_2 compression	
Number of intercooled compression stages	3
Intercooled compressor isentropic efficiency, %	85
Pressure at the last intercooled compressor/pump outlet, bar	80/110
CO_2 temperature at intercooler outlet, °C	25
Pump hydraulic efficiency, %	75

Nomenclature

AGR	Acid gas removal
ASU	Air separation unit
CAP	Chilled ammonia process
CCS	Carbon capture and storage
CT	Combustion turbine
ER	CO_2 emission rate, kg_{CO_2}/kWh
HP/LP/MP	High/low/medium pressure, bar
HRSC	heat recovery steam cycle
HRSG	heat recovery steam generator
LHV	Lower heating value, MJ/kg
IGCC	Integrated gasification combined cycle
$\dot{m}$	Mass flow rate, kg/s
$\dot{n}$	Molar flow rate, mol/s
OECD	Organisation for Economic Co-operation and Development
ref	Reference (power plant with no CO_2 capture)
SPECCA	Specific primary energy consumption for CO_2 avoided, MJ/kg_{CO_2}
η	Efficiency

References

[1] Cui X, Hong J, Gao M. Environmental impact assessment of three coal-based electricity generation scenarios in China. Energy 2012;45(1):952−9.

[2] Zhang H, Zhang B, Bi J. More efforts, more benefits: air pollutant control of coal-fired power plants in China. Energy 2015;80(1):1−9.

[3] Shrivastava N, Sharma S, Chauhan K. Efficiency assessment and benchmarking of thermal power plants in India. Energy Policy 2012;40:159−76.

[4] Guttikunda SK, Jawahar P. Atmospheric emissions and pollution from the coal-fired thermal power plants in India. Atmos Environ 2014;92:449−60.

[5] Chou CL. Sulfur in coals: a review of geochemistry and origins. Int J Coal Geol 2012;100:1−13.

[6] Baruya P. Coal contracts and long-term supplies, IEA clean coal centre report CCC/258, ISBN 978-92-9029-581-5. http://www.iea-coal.org.uk/.

[7] Cau G, Tola V, Bassano C. Performance evaluation of high-sulphur coal-fired USC plant integrated with SNOX and CO_2 capture sections. Appl Therm Eng 2015;74:136−45.

[8] Wang B, Xiao G, Song X, Zhao H, Zheng C. Chemical looping combustion of high-sulfur coal with $NiFe_2O_4$-combined oxygen carrier. J Therm Anal Calorim 2014;118:1593−602.

[9] Pettinau A, Dobó Z, Köntös Z, Zsemberi A. Experimental characterization of a high sulfur Hungarian brown coal for its potential industrial applications. Fuel Process Technol 2014;122:1−11.

[10] Ishibashi Y, Shinada O. First year operation results of CCP's Nakoso 250MW air-blown IGCC demonstration plant. In: Gasification Technologies Confer-ence; 2008. Washington, DC, USA.

[11] Giuffrida A, Romano MC, Lozza G. Thermodynamic analysis of air-blown gasification for IGCC applications. Appl Energy 2011;88(11):3949−58.

[12] Giuffrida A, Romano MC, Lozza G. Efficiency enhancement in IGCC power plants with air-blown gasification and hot gas clean-up. Energy 2013;53: 221−9.

[13] Olajire AA. CO_2 capture and separation technologies for end-of-pipe applica-tions − a review. Energy 2010;35(6):2610−28.

[14] Sreenivasulu B, Gayatri DV, Sreedhar I, Raghavan KV. A journey into the process and engineering aspects of carbon capture technologies. Renew Sustain Energy Rev 2015;41:1324−50.

[15] Damen K, Gnutek R, Kaptein J, Nannan NR, Oyarzun B, Trapp C, et al. De-velopments in the pre-combustion CO_2 capture pilot plant at the Buggenum IGCC. Energy Procedia 2011;4:1214−21.

[16] Giuffrida A, Bonalumi D, Lozza G. Amine-based post-combustion CO_2 capture in air-blown IGCC systems with cold and hot gas clean-up. Appl Energy 2013;10:44−54.

[17] Bonalumi D, Giuffrida A, Lozza G. A study of CO_2 capture in advanced IGCC systems by ammonia scrubbing. Energy Procedia 2014;45:663−70.

[18] Kawabata M, Kurata O, Iki N, Tsutsumi A, Furutani H. System modeling of exergy recuperated IGCC system with pre- and post-combustion CO_2 capture. Appl Therm Eng 2013;54(1):310−8. http://dx.doi.org/10.1016/j.applthermaleng.2013.01.029.

[19] Asif M, Bak CU, Saleem MW, Kim WS. Performance evaluation of integrated gasification combined cycle (IGCC) utilizing a blended solution of ammonia and 2-amino-2-methyl-1-propanol (AMP) for CO_2 capture. Fuel 2015;160: 513−24. http://dx.doi.org/10.1016/j.fuel.2015.08.008.

[20] Budzianowski WM. CO_2 reactive absorption from flue gases into aqueous ammonia solutions: the NH_3 slippage effect. Environ Prot Eng 2011;37(4): 5−19.

[21] Black S, Paelinck P, Kozak F, Petig A, Morris E. Chilled ammonia process for CO_2 capture. In: Proceedings of Pennwell oil sands conference, Calgary, Alberta, Canada; 2008.

[22] EIG Inc, Ultra cleaning of combustion gas including the removal of CO2, WO Patent No WO/2006/022885 (2006).

[23] Bollinger R, Muraskin D, Hammond M, Kozak F, Spitznogle G, Cage M, et al. CCS Project with Alstom's chilled ammonia process at AEP's mountaineer plant. Technical report of ALSTOM Power Systems. 2010. p. 1−19. http://www.mcilvainecompany.com/Decision_Tree/subscriber/CO2DescriptionTextLinks/AlstomMountaineer.pdf.

[24] Mathias PM, Reddy S, O'Connell JP. Quantitative evaluation of the chilled-ammonia process for CO_2 capture using thermodynamic analysis and pro-cess simulation. Int J Greenh Gas Control 2010;4(2):174−9. http://dx.doi.org/10.1016/j.ijggc.2009.09.016.

[25] Versteeg P, Rubin ES. A technical and economic assessment of ammonia-based post-combustion CO_2 capture at coal-fired power plants. Int J Greenh Gas Control 2011;5(6):1596−605. http://dx.doi.org/10.1016/j.ijggc.2011.09.006.

[26] Yu H, Morgan S, Allport A, Cottrell A, Do T, McGregor J, et al. Results from trialling aqueous NH_3 based post-combustion capture in a pilot plant at Munmorah power station: absorption. Chem Eng Res Des 2011;89(8): 1204−15. http://dx.doi.org/10.1016/j.cherd.2011.02.036.

[27] Yu H, Qi G, Wang S, Morgan S, Allport A, Cottrell A, et al. Results from trialling aqueous ammonia-based post-combustion capture in a pilot plant at Mun-morah power station: gas purity and solid precipitation in the stripper. Int J Greenh Gas Control 2012;10:15−25. http://dx.doi.org/10.1016/j.ijggc.2012.04.014.

[28] Lombardo G, Agarwal R, Askander J. Chilled ammonia process at technology center Mongstad − first results. Energy Procedia 2014;51:31−9.

[29] http://www.tcmda.com/en/Press-center/News/2015/Alstom-continues-development-of-CCS-technologies/.

[30] Sutter D, Gazzani M, Mazzotti M. Formation of solids in ammonia-based CO_2 capture processes — Identification of criticalities through thermodynamic analysis of the CO_2−NH_3−H_2O system. Chem Eng Sci 2015;133:170−80. http://dx.doi.org/10.1016/j.ces.2014.12.064.

[31] Valenti G, Bonalumi D, Macchi E. Modeling ultra super critical power plants integrated with the chilled ammonia process. Energy Procedia 2011;4: 1721−8.

[32] Valenti G, Bonalumi D, Macchi E. A parametric investigation of the chilled ammonia process from energy and economic perspectives. Fuel 2012;101:74−83.

[33] Valenti G, Bonalumi D, Fosbøl P, Macchi E, Thomsen K, Gatti D. Alternative layouts for the carbon capture with the chilled ammonia process. Energy Procedia 2013;37:2076−83.

[34] http://www.phasediagram.dk/.

[35] Thomsen K, Rasmussen P. Modeling of vapor-liquid-solid equilibrium in gas-aqueous electrolyte systems. Chem Eng Sci 1999;54:1787−802.

[36] Darde V, Thomsen K, van Well WJM, Stenby EHS. Modeling of carbon dioxide absorption by aqueous ammonia solutions using the Extended UNIQUAC model. Ind Eng Chem Res 2010;49:12663−74.

[37] Abrams DS, Prausnitz JM. Statistical thermodynamics of liquid mixtures: a new expression for the excess Gibbs energy of partly or completely miscible systems. AIChE J 1975;21:116−28.

[38] Maurer G, Prausnitz JM. Derivation and extension of the UNIQUAC equation. Fluid Phase Equilib 1978;2:91.

[39] Darde V, Thomsen K, van Well WJM, Bonalumi D, Valenti G, Macchi E. Com-parison of two electrolyte models for the carbon capture with aqueous ammonia. Int J Greenh Gas Control 2012;8:61−72. http://dx.doi.org/10.1016/j.ijggc.2012.02.002.

[40] Bonalumi D, Giuffrida A. Post-combustion CO_2 capture by aqueous ammonia in an advanced IGCC fired with high-sulphur coal. In: Proceedings of ECOS 2015, June 30-July 3; 2015. Pau, France.

[41] http://www.gecos.polimi.it/software/gs.php.

[42] Chiesa P, Macchi E. A thermodynamic analysis of different options to break 60% electric efficiency in combined cycle power plants. J Eng Gas Turbine Power 2004;126(4):770−85.

[43] Giuffrida A, Romano MC, Lozza G. Thermodynamic assessment of IGCC power plants with hot fuel gas desulfurization. Appl Energy 2010;87(11): 3374−83.

[44] Giuffrida A, Romano MC. On the effects of syngas clean-up temperature in IGCCs. In: Proceedings of ASME Turbo Expo 2010; 2010 June 14-18. http://dx.doi.org/10.1115/GT2010-22752. Glasgow, UK.

[45] Giuffrida A, Romano MC, Lozza G. CO_2 capture from air-blown gasification-based combined cycles. In: Proceedings of ASME Turbo Expo 2012; 2012 June 11-15. http://dx.doi.org/10.1115/GT2012-69787. Copenhagen, Denmark.

[46] Moioli S, Giuffrida A, Gamba S, Romano MC, Pellegrini L, Lozza G. Pre-com-bustion CO_2 capture by MDEA process in IGCC based on air-blown gasification. Energy Procedia 2014;37:2045−53.

[47] Giuffrida A. Impact of low-rank coal on air-blown IGCC performance. In: Proceedings of ASME Turbo Expo 2014; 2014 June 16-20. http://dx.doi.org/10.1115/GT2014-26843. Düsseldorf, Germany.

[48] Giuffrida A, Moioli S, Romano MC, Lozza G. Lignite-fired air-blown IGCC sys-tems with pre-combustion CO_2 capture. Int J Energy Res 2016;40(6):831−45. http://dx.doi.org/10.1002/er.3488.

[49] Kurz F, Rumpf B, Maurer G. Vapor-liquid-solid equilibria in the system NH_3-CO_2-H_2O from around 310 to 470 K: new experimental data and modeling. Fluid Phase Equilib 1995;104:261−75.

[50] Bonalumi D, Valenti G, Lillia S, Fosbøl P, Thomsen K. A layout for the carbon capture with aqueous ammonia without salt precipitation. Energy Procedia 2016;86:134–43. http://dx.doi.org/10.1016/j.egypro.2016.01.014.

[51] Hashimoto T., Ota K., Fujii T., Progress update for commercial plants of air blown IGCC. Proceedings of ASME Turbo Expo 2007; vol. 1:499–504. doi: 10.1115/GT2007-28348.

[52] European best practice guidelines for assessment of CO_2 capture technologies − Available at: <http://caesar.ecn.nl/fileadmin/caesar/user/documents/D_4.9_best_practice_guide.pdf>.

[53] Chiesa P, Lozza G, Mazzocchi L. Using hydrogen as gas turbine fuel. J Eng Gas Turbine Power 2005;127(1):73–80. http://dx.doi.org/10.1115/1.1787513.

[54] Kunze C, Spliethoff H. Modelling, comparison and operation experiences of entrained flow gasifier. Energy Convers Manag 2011;52(5):2135–41.

[55] Spallina V, Romano MC, Chiesa P, Gallucci F, van Sint Annaland M, Lozza G. Integration of coal gasification and packed bed CLC for high efficiency and near-zero emission power generation. Int J Greenh Gas Control 2014;27:28–41.

[56] Gargurevich IA. Hydrogen sulfide combustion: relevant issues under Claus furnace conditions. Ind Eng Chem Res 2005;44:7706–29.

[57] Korens N, Simbeck DR, Wilhelm DJ. Process screening analysis of alternative gas treating and sulfur removal, SFA Pacific for U.S. Department of Energy. Mountain View, CA. December 2002.

[58] Asadi S, Pakizeh M, Chenar MP. An investigation of reaction furnace temperatures and sulfur recovery. Front Chem Sci Eng 2011;5(3):362–71. http://dx.doi.org/10.1007/s11705-011-1106-z.

[59] Kvamsdal HM, Romano MC, van der Ham L, Bonalumi D, van Os P, Goetheer E. Energetic evaluation of a power plant integrated with a piperazine-based CO_2 capture process. Int J Greenh Gas Control 2014;28:343–55.

[60] Bonalumi D, Ciavatta A, Giuffrida A. Thermodynamic assessment of cooled and chilled ammonia-based CO_2 capture in air-blown IGCC plants. Energy Procedia 2016;86:272–81. http://dx.doi.org/10.1016/j.egypro.2016.01.028.